Indian Journal of Experimental Biology
Vol. 58, April 2020, pp. 263-270

Antimycotic activity of biogenically synthesised metal and metal oxide nanoparticles against plant pathogenic fungus *Fusarium moniliforme* (*F. fujikuroi*)

Anu Kalia[1]*, Jaspal Kaur[2], Amrinder Kaur[3] & Narinder Singh[3]

[1]Electron Microscopy and Nanoscience Laboratory, Department of Soil Science; [2]Department of Plant Breeding and Genetics; [3]Department of Plant Pathology; Punjab Agricultural University, Ludhiana, Punjab-141 004, India

Received 10 May 2019; *revised 23 September 2019*

Consistent and injudicious application of antifungal agents to control fungal pathogens on crops results in off-target ill-effects on livestock and human health besides issues, such as disruption of ecological balance. In this context, development of novel specific antifungal agents such as metal or metal oxide nanoparticles without side effects becomes a necessity. Here, we attempted green synthesis of three different metal and metal oxide nanoparticles (NPs) (Ag, ZnO and FeO) by incubating metal salts with *Trichoderma harzianum* hyphal or mycelial extract (HE). The AgNPs were also generated using hyphal filtrate (HF). The synthesized nanoparticles were characterized by microscopy and spectroscopy techniques and evaluated by poisoned food technique/agar well diffusion technique under *in vitro* conditions on Czapek dox agar against plant pathogenic fungus *Fusarium moniliforme*. The tested NPs exhibited varied efficacy for curbing the growth of *F. moniliforme.* A NP concentration dependent increase in percent growth inhibition was recorded for the above mentioned three types of NPs. Moreover, the antimycotic efficacy of the microbial synthesized Ag NPs also varied for the *T. harzianum* cell free filtrate and hyphal extract formulations. Maximum percent hyphal growth inhibition (58.83%) was recorded for *T. harzianum* HE Ag NPs at 800 ppm followed by FeO NPs at 400 ppm (40.38%).

Keywords: Antifungal, Basmati foot-rot disease, Myconanoparticles, Poison food assay, *Trichoderma* spp.

Plant pathogens inflict huge economic losses by infection and disease in crop plants[1]. These plant diseases can be managed by employing different conventional management practices, such as cultural, physical, biological and chemical strategies[2]. However, each strategy has its own advantage and associated disadvantages[3]. Chemical management is one of the most extensively used methods of disease management though it suffers from incidences of development of resistance due to non-targeted delivery. The biological strategies are time-consuming and vary in their field efficacy[4]. Currently, nanotechnology is emerging as a potential strategy in disease management of crops[5].

Nanotechnology involves synthesis, characterization and application of engineered nanomaterials including nanoparticles (NPs). These nanomaterials behave differently from the bulk which makes them interesting materials for diverse applications[6]. There are several approaches for synthesis of NMs including physical (attrition, miling and laser/electron etching), chemical (sol gel techniques), and combined physicochemical and biological techniques. The biological synthesis of NPs is the most cost effective and environmentally friendly technique. Plenty of reports are available on synthesis of NPs using plant[7], plant extracts[8] and microbes such as bacteria[9,10], fungus[11] and algae.

Among the NPs synthesized and characterized, the inorganic metal and metal oxide NPs viz. Ag[9], ZnO[12], FeO[13], MgO[14], and TiO_2[15] have been known to possess potent antimicrobial activities due to their selective toxicity to biological system[7]. However, there are limited reports available on evaluation of antimycotic activity of metal/metal oxide NPs[16-19]. In the present study, we tried to evaluate antifungal activity of Ag, FeO and ZnO nanoparticles against plant pathogenic *Fusarium moniliforme* causing foot rot disease in basmati rice.

Materials and Methods

Three metal salts i.e., silver nitrate ($AgNO_3$), zinc sulphate ($ZnSO_4$) and ferric chloride ($FeCl_3$) used for the NP synthesis were procured from Merck India Pvt. Ltd, India. The analytical grade prepared media, Czapek dox agar and potato dextrose agar utilized for the growth and maintenance of fungal cultures were

*Corresponding:
E-mail: kaliaanu@pau.edu, kaliaanu@gmail.com

procured from HiMedia Laboratories Pvt. Ltd, Mumbai, India. The fungal cultures i.e., *Trichoderma harzianum* and *Fusarium moniliforme* were procured from culture collection maintained by the Department of Plant Pathology, PAU, Ludhiana, Punjab, India.

The green synthesis of Ag, ZnO and FeO nanoparticles was carried using hyphal extract (HE) and culture filtrate (HF) of potential biocontrol agent *Trichoderma harzianum* as per the modified protocol[20,21]. The fungal biomass was prepared by growing active culture in Czapek dox media comprised of g L^{-1}: sucrose (30.0), sodium nitrate (2.0), dipotassium phosphate (1.0), magnesium sulphate (0.5), potassium chloride (0.5), ferrous sulphate (0.01), pH (at 25°C) was set at 7.3±0.2°C. The inoculated media was incubated at 27±2°C in shaker-cum-incubator at a shaking speed of 160 rpm for 72 h. The fungal biomass was filtered through Whatman filter paper no. 1 using negative pressure in a vacuum filtration assembly. The filtered fungal biomass was washed thoroughly with deionized water. Then the collected biomass (known wet weight basis) was resuspended in deionized distilled water (250 mL) and incubated at 25±2°C with continuous shaking (160 rpm) for 72 h. The fungal biomass was again filtered to obtain the cell-free extract[11,12].

Another assembly was also maintained containing only the liquid broth in which fungus was cultured. The fungal biomass after growth was filtered to obtain the hyphal filtrate. Both the hyphal extract and the hyphal filtrate were incubated with 1.0 mM silver nitrate[11] while only hyphal extract was incubated with 1.0 mM zinc sulphate[12] and iron chloride salts in equal ratio (1:1) at 27±2°C under shaking conditions (160 rpm) to synthesize nanoparticles. For all the metal salts a positive (HF and HF without metal salt) and negative (1.0 mM $AgNO_3$, $ZnSO_4$ and $FeCl_3$ solutions) control were also maintained at same temperature and shaking conditions. The visual characterization of the NP synthesis was documented as appearance/difference in colour of the suspension that was monitored after every hour. A colour change in silver and FeO NP solutions was indicative of synthesis of NPs while the ZnO NPs suspensions remained transparent.

The synthesized NPs were characterized by spectroscopy and microscopy tools. The NP suspensions were analyzed for the specific UV absorption peaks indicating the synthesis of NPs by performing UV-Vis spectroscopy[11] measurements that were recorded on a Shimadzu dual-beam spectrophotometer (model UV-1601 PC) operated at a resolution of 1.0 nm.

Further, the morphological characterization of the synthesized NPs was performed by Electron Microscopy (EM) of the samples. The SEM study of various NP suspensions was performed under SE imaging mode (model Hitachi s-3400N, Japan)[12]. While the SEM-Energy Dispersive X-ray Spectroscopy (SEM-EDS) analysis to determine the elemental composition of sample was performed using EDS (model Thermo Noran System Six, USA) attached to SEM[12]. The size of NPs was determined by viewing the drop casted NP suspensions in high contrast mode at high magnifications of X20000 to X40000 in TEM (model Hitachi H-7650, Japan) operating at an accelerating voltage of 80 kV[8,11,12]. The hydrodynamic size (in nm), zeta potential (ζ) and polydispersity index (PDI) of the aqueous nanoparticle suspensions pre-sonicated for 30 min in bath sonicator assembly (model Toshniwal, India) were studied in a DLS-Zeta-sizer (model Malvern Zetasizer Nano, UK)[8].

The Fourier Transform Infra Red Spectroscopy (FT-IRS) of silver nanoparticles was also performed to characterize the presence of characteristic absorption peaks indicating presence of specific functional groups by drying 1.0 mL of NP suspension in oven at 40°C followed by mixing with and preparation of potassium bromide pellets[11]. The pellets were studied in Thermo FT-IR-NXT-Raman Spectroscope and a spectrum was obtained in the mid IR region at 4000 to 400 cm^{-1} wave numbers.

After characterization, the synthesized NP formulations were bioassayed for their effect on colony growth of *F. moniliforme* at different working concentrations (0-800 ppm) by poisoned food technique on Czapek Dox medium. The 5 mm discs of pure culture of *F. moniliforme* were cut using cork borer and placed in the centre of the solidified Czapek Dox plates in each of the concentration under aseptic conditions and thereafter incubated at 25±2°C. A separate Petri plate in each case containing only Czapek Dox medium served as control. Each treatment was replicated thrice. Radial growth of the pathogen was measured after 3 and 5 days of

incubation and colony growth inhibition was calculated using the formula:

$$Colony\ growth\ inhibition = \frac{c-T}{c} \times 100$$

where C is, growth of the pathogen in control; and T is the growth of the pathogen in treatment.

Results

Synthesis of silver, zinc oxide and iron oxide nanoparticles

The green synthesis of Ag, ZnO and FeO nanoparticles in this experiment involved reduction of metal salts by biological macromolecules excreted by the cells or diffused out of the *Trichoderma harzianum* cells/hyphae by incubation with the fungal biomass in deionised water in presence of light. The NPs thus formed were observed to exhibit specific optical colour properties such as appearance of red brown colour due to surface plasmon resonance of silver NPs (Ag NPs) (Fig. 1) while the zinc oxide solution remained transparent and later showed formation of white precipitates on continued incubation.

Characterization of nanoparticle solutions

UV-Vis spectroscopy

The UV-Vis spectra recorded from the *Trichoderma harzianum* reaction vessel supplemented with 1.0 mM $AgNO_3$ solution at two different reaction times is depicted in Fig. 2. This UV-Vis spectrum of the biologically synthesized Ag nano-solution indicated the presence of characteristic surface plasmon band that appeared at 420 nm. The results also indicate increase in intensity of SPR peak of the Ag NP sol with time indicating continued nucleation, formation and aggregation of Ag NPs in the aqueous phase. On the other hand, ZnO NP solution did not exhibit any sharp and specific UV-Vis spectra probably due to the transparent nature of the solution.

Electron Microscopy and Energy Dispersive X-ray spectroscopy

The SEM of the three nano-solutions depicted the formation of crystallites of size less than 100 nm. However, the good contrast images of NPs were observed only for hyphal extract derived Ag solutions in HR-SEM (Fig. 3). The SEM-EDS of the solutions confirmed the presence of Ag, Zn, and Fe elements in respective solutions. Interestingly, the Ag solutions synthesized by incubating *T. harzianum* biomass in hypotonic solution (HE) exhibited occurrence of Ag element content (atom and weight %) higher than the hyphal filtrate (HF) generated Ag NP solutions (Fig. 4).

Fig. 1 — Visual observation of *Trichoderma harzianum* biomass (A) before and (B) after exposure to Ag^+ ions. The dark reddish brown colour indicates the formation of AgNPs; and (C) deionized water with $AgNO_3$ salt.

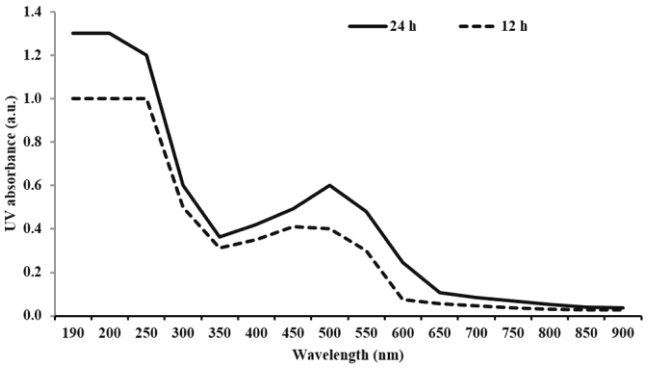

Fig. 2 — UV-Vis spectroscopy of nano-Ag sols synthesized by incubation of $AgNO_3$ salt with hyphal extract of *Trichoderma harzianum* at different time intervals

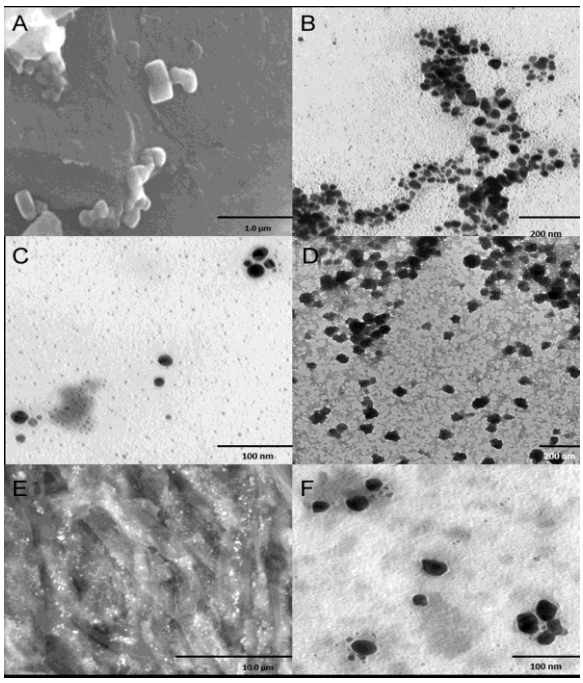

Fig. 3 — SEM and High contrast TEM of different metal and metal oxide nanoparticles biologically synthesized from *Trichoderma harzianum.* (A) SEM of Ag NPs (HE) (X30000); (B) TEM of Ag NPs (HE) (X20000); (C) TEM of Ag NPs (HF) (X50000); (D) TEM of FeO NPs (X12000); (E) SEM of ZnO NPs attached to fungal hyphae (X5000); and (F) TEM of ZnO NPs (X50000)

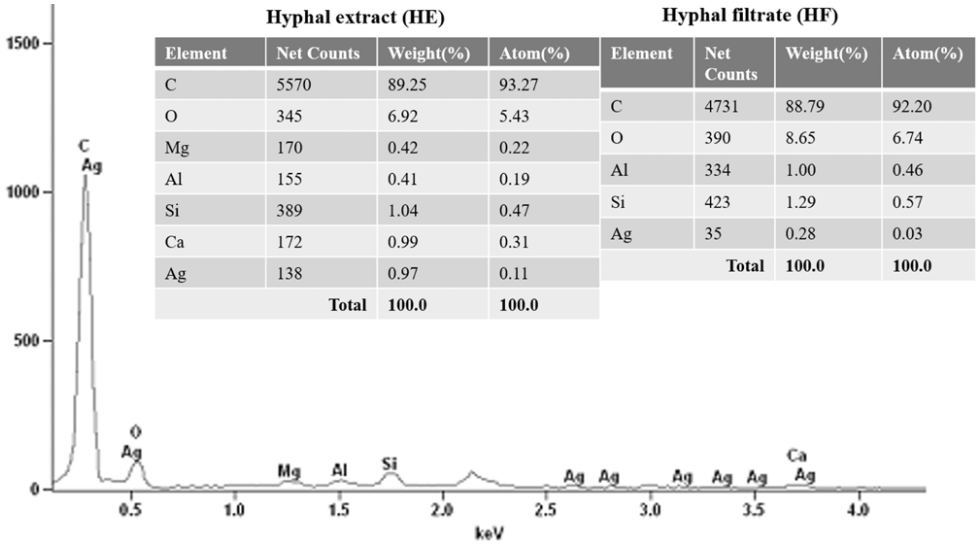

Fig. 4 — SEM-Energy Dispersive X-ray Spectroscopy of Ag NPs synthesized by *Trichoderma harzianum* hyphal extract and filtrate

Table 1 — Hydrodynamic size, zeta potential and polydispersity index of biosynthesized nanoparticles

Source	Nanoparticle	Hydrodynamic size (nm)	Zeta potential (ζ) (mV)	Polydispersity index
Hyphal filtrate	Ag NPs	63.10±7.01	–16.23	0.366
Hyphal extract	Ag NPs	4.01±0.25	–19.17	0.211
	ZnO NPs	111.53±1.3	–15.89	0.465
	FeO NPs	81.73±3.0	–10.83	0.875

The TEM of the drop casted Ag, ZnO and FeO NPs showed the presence of nanoparticles with variable shape and size, dispersed or aggregated and appear to be embedded in a gelatinous matrix probably due to coating of the nanoparticle surface with the extracellular macromolecules synthesized and released by the fungal biomass (Fig. 3). The average size of NPs ranged from 5-50, 20-60 and 10-40 nm for Ag, FeO and ZnO NPs, respectively.

Dynamic Light Scattering Spectroscopy and Zeta potential

The synthesized nanoparticle sols (Ag, ZnO and FeO NPs) obtained by HE and Ag nanosols (Ag NPs) obtained from HF on DLS analysis exhibited occurrence of variable hydrodynamic size of nanoparticles (Table 1) with HE derived Ag NPs having the smallest hydrodynamic diameter (4.01±0.25 nm). Further, all the generated nanosols showed negative average zeta potential values while the polydispersity indices varied with particularly higher values for FeO NPs (Table 1).

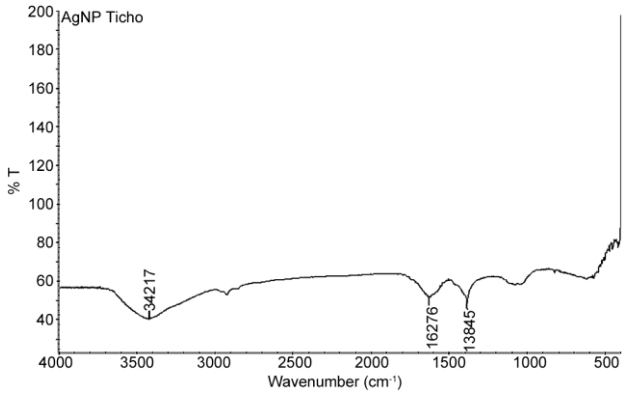

Fig. 5 — FTIR spectroscopy of *Trichoderma* generated Ag NPs

Fourier Transform Infra Red Spectroscopy (FT-IRS)

The FT-IR spectrum of the *Trichoderma* synthesized Ag NPs showed the absorption peaks at 3421, 1627, and 1384 cm^{-1} due to N-H bond bending indicating the primary and secondary amine groups of protein and carbonyl stretching vibrations of protein, respectively (Fig. 5). These bending and stretching vibrations of the N-H and C-H bonds indicate the stronger metal-binding capability of the carbonyl group of amino acid residues and peptides of proteins.

Antimycotic activity assay

Antimycotic activity of the synthesized nanoparticles was assayed by amending culture medium with different concentrations of the NPs and colony diameter of the fungus was recorded at 24 h intervals. All the test nanoparticles varied in the extent of inhibition of the colony growth of *F. moniliforme* at different concentrations and statistically differed

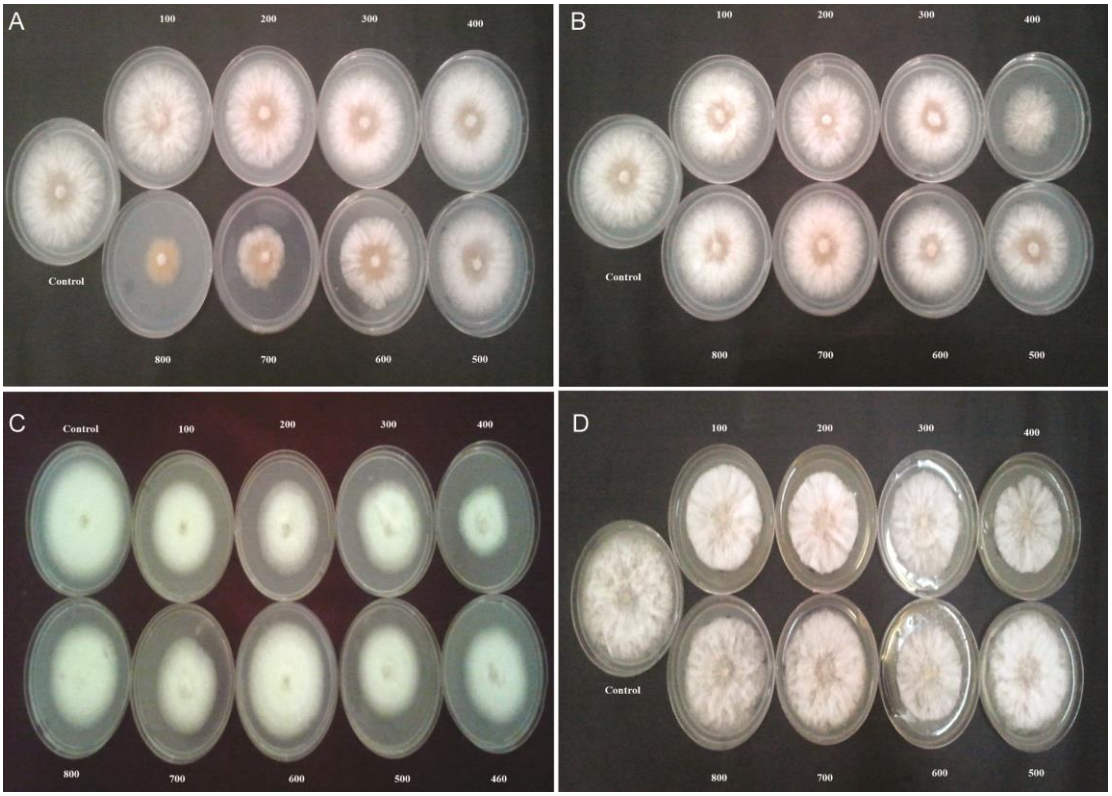

Fig. 6 — Effect of different concentrations of metal and metal oxide nanoparticles (in ppm) synthesized by *Trichoderma harzianum* on colony growth of *Fusarium* after three days of incubation in Czapek Dox agar. (A) Ag NPs (hyphal extract); (B) Ag NPs (hyphal filtrate); (C) FeO NPs; and (D) ZnO NPs

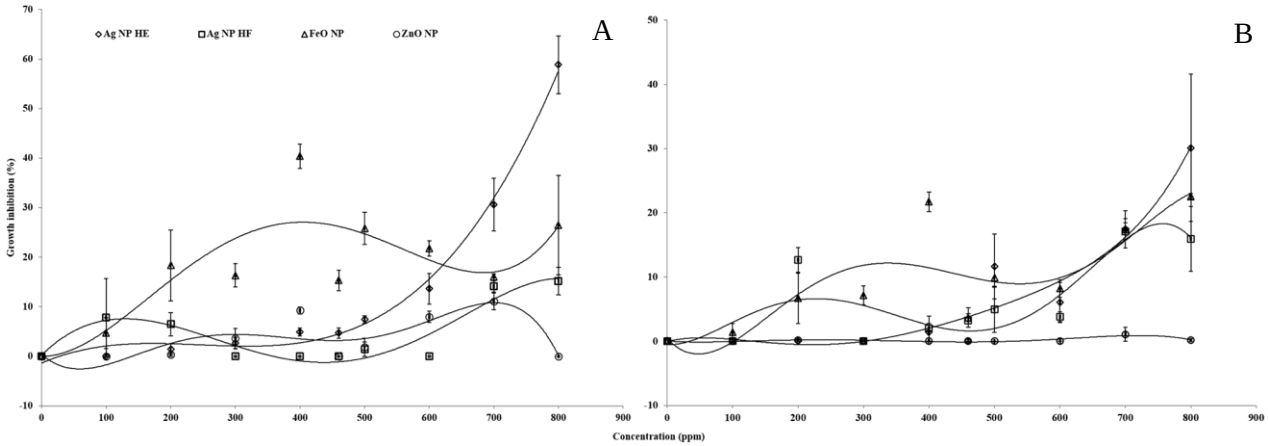

Fig. 7 — Effect of different metal and metal oxide nanoparticles on growth inhibition (%) of *Fusarium* at (A) 3; and (B) 5 days of incubation under *in vitro* conditions. [Values are presented as means ± standard errors]

significantly from each other (Fig. 6). The data is presented only for inhibition in colony growth of *F. moniliforme* after 3 and 5 days of incubation. Maximum inhibition in colony growth diameter under *in vitro* conditions was observed in Ag NPs synthesized using *T. harzianum* mycelial extracts followed by FeO based NPs synthesized using *T. harzianum* culture filtrate. At 800 ppm, Ag NPs (HE) maximally inhibited the fungal growth i.e. 58.83% compared to nil inhibition in control. Direct correlation between the concentration of nanoparticles and extent of colony growth inhibition was observed in case of Ag NPs (HE). The FeO NPs at 400 ppm gave 40.38% colony growth inhibition followed by 30.62% inhibition shown by Ag NP (HE) at 700 ppm after three days of incubation (Fig. 7 A and B).

Discussion

Synthesis of silver, zinc oxide and iron oxide nanoparticles

Green or biogenically synthesized Ag and metal oxide NPs using *Trichoderma reesei*[22], *T. harzianum*[20], *T. viride*[23], *T. longibrachiatum*[24] and different species of *Trichoderma* have been documented[25]. The synthesis of Ag NPs observed as change in colour of the $AgNO_3$ solution to reddish brown on incubation in presence of light has been documented in published reports[22-27]. Zinc oxide[28,29] and iron oxide[30] nanoparticles can also be synthesized by incubating dissolved Zn/Fe salts with fungal cell extracts.

UV-Vis spectroscopy

Strong absorption peak for Ag nanosols myco-synthesized from cell extracts of fungi such as *Aspergillus fumigatus*[31], and particularly *Trichoderma*[24] have been reported to appear at 400 and 420 nm, respectively. However, the UV-Vis absorption maxima for Ag NPs may vary from 400 to 520 nm depending on the size and aggregation of the Ag NPs in the solution.

Electron Microscopy and Energy Dispersive X-ray spectroscopy

A similar size of Ag NPs ranging from 30-50 nm has been reported to be produced by *Trichoderma viride*[24]. Kaur *et al*.[11] also observed the polydisperse spherical and occasionally ellipsoid Ag NPs in the size range 10-50 nm synthesized by using macro-fungal hyphal extracts of *Pleurotus florida*. Likewise, ZnO NPs with a size of 9 to 17 nm have been reported on gamma irradiation of the hyphal extracts of *Penicillum chrysogenum*[28]. Unlike the results obtained in this study, the *Trichoderma asperellum* hyphae extract derived iron oxide nanoparticles had a size of 18 to 32 nm[30].

Dynamic Light Scattering Spectroscopy and zeta potential analysis

The physicochemical properties including hydrodynamic (HD) size, and charge distribution on NP surface affect the biodistribution and target of nanoparticles in biological milieu[32]. A similar size distribution and HD diameter have been observed[31]. Further, the stability of the nano-sols may be attributed to the surface charge at the slipping plane or the zeta potential of the constituent nanoparticles. The zeta potential values range from –30 to +30 mV such that a highly negative zeta value indicates huge electrostatic repulsive forces which counter-act the phenomena of nanoparticle agglomeration within the sol. Therefore, zeta potential is considered a useful attribute to indicate the stability of nano-dispersion[32]. Our results could be corroborated with that of Santos *et al*.[33] who have assessed that biosynthesized AgNPs exhibited zeta potential of –31.7 mV with PDI of 0.231.

Fourier Transform Infra Red Spectroscopy (FT-IRS)

Spectral peaks at specific wave numbers (3269.31, 2156.94 and 1634.92 cm^{-1}) indicating stretching vibrations of primary amines, and bending vibrations for amide I and II protein bonds were observed for Ag NPs synthesized by incubation of Ag salt with mycelia extract of *T. reesei*[24].

Antimycotic activity assay

Antifungal potential of NP formulations has been reported by several researchers, though, Ag NPs are predominantly known to possess higher inhibition potential against prokaryotic bacteria than eukaryotic fungi[23,24]. However, Elamawi *et al.*[24] compared the antimycotic potential of $AgNO_3$ solution *vs*. Ag NPs against nine plant pathogenic fungi in *in vitro* Petri dish assay. They have reported significant reduction depicted as percent inhibition of mycelial radial growth on treatment with Ag NPs to range from 75.7-98.9% compared to 25.5-91.8% inhibition observed for $AgNO_3$ solution. The Ag NP size dependent superior inhibition of mycelial growth of *Sclerotinia sclerotiorum* has also been observed[27].

The ZnO NPs exhibit antifungal activity even at low concentrations[34]. Incubation of mycelial extracts with Zn salt substrate can lead to generation of ZnO NPs[29]. The antifungal potential of the fungus derived NPs can be performed both through poison food assay of agar media or in liquid broth culture. Broth culture study involving turbidimetric assessment showed that ZnO NPs moderately inhibited *A. alternata* and *B. cinerea* while a significantly high percent inhibition of *R. stolonifer* was observed[34]. Therefore, mycogenic derived ZnO NPs can also substantially inhibit fungal growth exhibiting high antifungal activity against several fungal cultures[28]. Mycelial growth and sporicidal or spore germination inhibiting potential of iron oxide NPs has also been documented[17]. The Fe_2O_3 nanoparticles showed significant antifungal activity against fungal pathogens including *Trichothecium roseum, Cladosporium herbarum, Penicillium chrysogenum, Alternaria alternata* and *Aspergillus niger*[17].

Conclusion

The biocontrol agent, *Trichoderma harzianum* can be utilized for rapid and green synthesis of stable formulations of metal or metal oxide NPs possessing

negative zeta potential values. The nano-dimensional range of the generated Ag (5-50 nm), ZnO (20-60 nm) and FeO (10-40 nm) particles as confirmed by UV-Vis spectroscopy and Electron microscopy (SEM and TEM) analysis. The nano-scale dimensions of the synthesized NPs had an impact on the anti-fungal activity against test *Fusarium* culture in this study. Specifically, on third day of incubation, Ag NPs (HE) (at 800 ppm) exhibited inhibition of radial mycelial growth of *Fusarium moniliforme* (more than 50%) while FeO NPs at half the concentration (i.e. at 400 ppm) showed ~40% inhibition in *in vitro* poison food assay. Thus, early and effective curbing of the fungal growth depends on both the size dimensions and concentration of the NPs used. Therefore, the antimycotic potential of the metal and metal oxide NPs can possibly be exploited for the management of plant pathogenic fungi.

Acknowledgement

The authors are thankful to the ICAR, New Delhi, for funding under the Nanotechnology Platform scheme.

Conflict of interest

The authors declare no conflict of interests.

References

1 Savary S, Willocquet L, Pethybridge SJ, Esker P, McRoberts N & Nelson A, The global burden of pathogens and pests on major food crops. *Nat Ecol Evol*, 3 (2019) 430.

2 He DC, Zhan JS & Xie LH, Problems, challenges and future of plant disease management: From an ecological point of view. *J Integr Agric*, 15 (2016) 705.

3 Dara SK, The New Integrated Pest Management Paradigm for the Modern Age. *J Integr Pest Manag*, 10 (2019) doi: 10.1093/jipm/pmz010

4 Köhl J, Kolnaar R & Ravensberg WJ, Mode of action of microbial biological control agents against plant diseases: Relevance beyond efficacy. *Front Plant Sci*, 10 (2019) 1.

5 Elmer W & White JC, The Future of Nanotechnology in Plant Pathology. *Annu Rev Phytopathol*, 56 (2018) 111.

6 Jeevanandam J, Barhoum A, Chan YS, Dufresne A & Danquah MK, Review on nanoparticles and nanostructured materials: History, sources, toxicity and regulations. *Beilstein J Nanotechnol*, 9 (2018) 1050.

7 Singh P, Kim YJ, Zhang D & Yang DC, Biological Synthesis of Nanoparticles from Plants and Microorganisms. *Trends Biotechnol*, 34 (2016) 588.

8 Kalia A, Manchanda P, Bhardwaj S & Singh G, Biosynthesized silver nanoparticles from aqueous extracts of sweet lime fruit and callus tissues possess variable antioxidant and antimicrobial potentials. *Inorg Nano-Metal Chem* (2020), DOI: 10.1080/24701556.2020.1735420.

9 Hamouda RA, Hussein MH, Abo-elmagd RA & Bawazir SS, Synthesis and biological characterization of silver nanoparticles derived from the cyanobacterium *Oscillatoria limnetica*. *Sci Rep*, 9 (2019) 1.

10 Kaur M, Kalia A & Thakur A, Effect of biodegradable chitosan-rice-starch nanocomposite films on post-harvest quality of stored peach fruit. *Starch/Staerke*, 69 (2017) 1.

11 Kaur G, Kalia A & Sodhi HS, Size controlled, time-efficient biosynthesis of silver nanoparticles from *Pleurotus florida* using ultra-violet, visible range, and microwave radiations. *Inorg Nano-Metal Chem*, 50 (2020) 35.

12 Kaur M & Kalia A, Role of salt precursors for the synthesis of zinc oxide nanoparticles and in imparting variable antimicrobial activity. *J Appl Nat Sci*, 8 (2016) 1039.

13 Pallela PNVK, Ummey S, Ruddaraju LK, Gadi S, Cherukuri CSL, Barla S & Pammi SVN, Antibacterial efficacy of green synthesized α-Fe_2O_3 nanoparticles using *Sida cordifolia* plant extract. *Heliyon*, 5 (2019) e02765.

14 Noori AJ & Kareem FA, The effect of magnesium oxide nanoparticles on the antibacterial and antibiofilm properties of glass-ionomer cement. *Heliyon*, 5 (2019) e02568.

15 Azizi-Lalabadi M, Ehsani A, Divband B & Alizadeh-Sani M, Antimicrobial activity of Titanium dioxide and Zinc oxide nanoparticles supported in 4A zeolite and evaluation the morphological characteristic. *Sci Rep*, 9 (2019) 1.

16 Devi HS, Boda MA, Shah MA, Parveen S & Wani AH, Green synthesis of iron oxide nanoparticles using *Platanus orientalis* leaf extract for antifungal activity. *Green Process Synth*, 8 (2019) 38.

17 Parveen S, Wani AH, Shah MA, Devi HS, Bhat MY & Koka JA, Preparation, characterization and antifungal activity of iron oxide nanoparticles. *Microb Pathog*, 115 (2018) 287.

18 Jamdagni P, Khatri P & Rana JS, Green synthesis of zinc oxide nanoparticles using flower extract of *Nyctanthes arbor-tristis* and their antifungal activity. *J King Saud Univ-Sci*, 30 (2018) 168.

19 Pariona N, Mtz-Enriquez AI, Sánchez-Rangel D, Carrión G, Paraguay-Delgado F & Rosas-Saito G, Green-synthesized copper nanoparticles as a potential antifungal against plant pathogens. *RSC Adv*, 9 (2019) 18835.

20 Prameela Devi T, Kulanthaivel S, Kamil D, Borah JL, Prabhakaran N & Srinivasa N, Biosynthesis of silver nanoparticles from *Trichoderma* species. *Indian J Exp Biol*, 51 (2013) 543.

21 Fayaz MA, Balaji K, Kalaichelvan PT & Venkatesan R, Fungal based synthesis of silver nanoparticles-An effect of temperature on the size of particles. *Colloids Surf B Biointerfaces*, 74 (2009) 123.

22 Gemishev OT, Panayotova MI, Mintcheva NN, Djerahov LP, Tyuliev GT & Gicheva GD, A green approach for silver nanoparticles preparation by cell-free extract from *Trichoderma reesei* fungi and their characterization. *Mater Res Express*, 6 (2019) 095040. https://doi.org/10.1088/2053-1591/ab2e6a

23 Elgorban AM, Al-Rahmah AN, Sayed SR, Hirad A, Mostafa AAF & Bahkali AH, Antimicrobial activity and green synthesis of silver nanoparticles using *Trichoderma viride*. *Biotechnol Biotechnol Equip*, 30 (2016) 299.

24 Elamawi RM, Al-Harbi RE & Hendi AA, Biosynthesis and characterization of silver nanoparticles using *Trichoderma longibrachiatum* and their effect on phytopathogenic fungi. *Egypt J Biol Pest Control*, 28 (2018) 1.

25 Guilger-Casagrande M & Lima R de, Synthesis of silver nanoparticles mediated by fungi: A review. *Front Bioeng Biotechnol*, 7 (2019) 1.

26 Guilger M, Pasquoto-Stigliani T, Bilesky-Jose N, Grillo R, Abhilash PC, Fraceto LF & De Lima R, Biogenic silver nanoparticles based on *Trichoderma harzianum*: Synthesis, characterization, toxicity evaluation and biological activity. *Sci Rep*, 7 (2017) 1.

27 Guilger-Casagrande M, Germano-Costa T, Pasquoto-Stigliani T, Fraceto LF & Lima R de, Biosynthesis of silver nanoparticles employing *Trichoderma harzianum* with enzymatic stimulation for the control of *Sclerotinia sclerotiorum*. *Sci Rep*, 9 (2019) 1.

28 Housseiny MM & Gomaa EZ, Enhancement of antimicrobial and antitumor activities of zinc nanoparticles biosynthesized by *Penicillium chrysogenum* AUMC 10608 using gamma radiation. *Egypt J Bot*, 59 (2019) 319.

29 Shamsuzzaman, Mashrai A, Khanam H & Aljawfi RN, Biological synthesis of ZnO nanoparticles using *C. albicans* and studying their catalytic performance in the synthesis of steroidal pyrazolines. *Arab J Chem*, 10 (2017) S1530.

30 Mahanty S, Bakshi M, Ghosh S, Chatterjee S, Bhattacharyya S, Das P, Das S & Chaudhuri P, Green synthesis of iron oxide nanoparticles mediated by filamentous fungi isolated from Sundarban Mangrove ecosystem, India. *Bionanoscience*, 9 (2019) 637.

31 Shahzad A, Saeed H, Iqtedar M, Hussain SZ, Kaleem A, Abdullah R, Sharif S, Naz S, Saleem F, Aihetasham A & Chaudhary A, Size-controlled production of silver nanoparticles by *Aspergillus fumigatus* BTCB10: Likely antibacterial and cytotoxic effects. *J Nanomater*, 2019 (2019).

32 Carvalho PM, Felício MR, Santos NC, Gonçalves S & Domingues MM, Application of light scattering techniques to nanoparticle characterization and development. *Front Chem*, 6 (2018) 1.

33 Santos LM, Stanisic D, Menezes UJ, Mendonça MA, Barral TD, Seyffert N, Azevedo V, Durán N, Meyer R, Tasic L & Portela RW, Biogenic silver nanoparticles as a post-surgical treatment for *Corynebacterium pseudotuberculosis* infection in small ruminants. *Front Microbiol*, 10 (2019) 1.

34 Sardella D, Gatt R & Valdramidis VP, Turbidimetric assessment of the growth of filamentous fungi and the antifungal activity of zinc oxide nanoparticles. *J Food Prot*, 81 (2018) 934.